This document is the accepted manuscript version of the following article:
Hopper, T. R., Gorodetsky, A., Jeong, A., Krieg, F., Bodnarchuk, M. I., Maimaris, M., … Bakulin, A. A. (2020). Hot carrier dynamics in perovskite nanocrystal solids: role of the cold carriers, nanoconfinement, and the surface. Nano Letters, 20(4), 2271-2278. https://doi.org/10.1021/acs.nanolett.9b04491

# Hot Carrier Dynamics in Perovskite Nanocrystal Solids: Role of the cold carriers, nanoconfinement and the surface

*Thomas R. Hopper[†], Andrei Gorodetsky[†], Ahhyun Jeong[†], Franziska Krieg[‡¶], Maryna I. Bodnarchuk[‡¶], Marios Maimaris[†], Marine Chaplain[†], Thomas J. Macdonald[†], Xiaokun Huang[§#⊥], Robert Lovrincic[§#], Maksym V. Kovalenko[‡¶] and Artem A. Bakulin[†*]*

[†]Department of Chemistry, Imperial College London, London W12 0BZ, United Kingdom

[‡]Institute of Inorganic Chemistry, Department of Chemistry and Applied Biosciences, ETH Zürich, CH-8093 Zürich, Switzerland

[¶]Laboratory for Thin Films and Photovoltaics, Empa − Swiss Federal Laboratories for Materials Science and Technology, CH-8600 Dübendorf, Switzerland

[§]Institute for High-Frequency Technology, Technische Universität Braunschweig, Schleinitzstrasse 22, 38106 Braunschweig, Germany

[#]InnovationLab, Speyerer Strasse 4, 69115 Heidelberg, Germany

[⊥]Kirchhoff Institute for Physics, University of Heidelberg, 69120 Heidelberg, Germany

* E-mail: a.bakulin@imperial.ac.uk

KEYWORDS: Perovskite nanocrystals, carrier cooling, electron-phonon coupling, ultrafast spectroscopy

Carrier cooling is of widespread interest in the field of semiconductor science. It is linked to carrier-carrier and carrier-phonon coupling, and has profound implications for the photovoltaic performance of materials. Recent transient optical studies have shown that a high carrier density in lead-halide perovskites (LHPs) can reduce the cooling rate through a "phonon bottleneck". However, the role of carrier-carrier interactions, and the material properties that control cooling in LHPs, are still disputed. To address these factors, we utilize ultrafast "pump-push-probe" spectroscopy on LHP nanocrystal (NC) films. We find that the addition of cold carriers to LHP NCs increases the cooling rate, competing with the phonon bottleneck. By comparing different NCs and bulk samples, we deduce that the cooling behavior is intrinsic to the LHP composition, and independent of the NC size or surface. This can be contrasted with other colloidal nanomaterials, where confinement and trapping considerably influence the cooling dynamics.

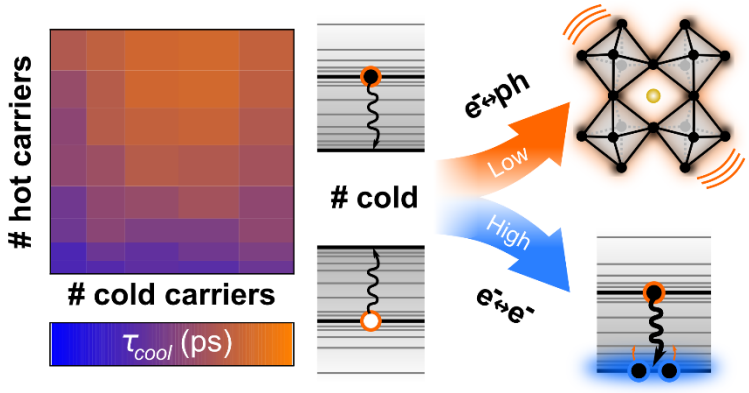

Lead-halide perovskite (LHP) nanocrystals (NCs) have recently emerged as highly encouraging materials for energy and photonic applications.[1] Their facile synthesis,[2] size-, shape- and composition-tunable optical properties,[3] high-performance emission characteristics[4–6] and purported "defect tolerance"[7,8] have prompted numerous studies into their fundamental photophysics. In particular, there is a concerted interest in two key types of interaction which govern the dynamics of charge carriers in these materials; (i) the interaction between carriers (e.g. carrier-carrier scattering[9–11] electron-hole correlation,[12,13] many-body recombination,[14–16] dielectric screening[17–19]) and (ii) the interactions between the carriers and the surrounding lattice (e.g. electron-phonon coupling,[20–23] polaron formation,[24–27] phase transitions,[28,29] anharmonicity[30–32]).

Both carrier-carrier and carrier-phonon interactions are known to mediate the relaxation of high-energy "hot" carriers in semiconductors.[33] A long-standing and ongoing aspiration of the photovoltaic community is to utilize these hot carriers prior to relaxation as a means to overcome the Shockley-Queisser limit for single-junction solar cells.[34] The main conceptual strategies for achieving this include either the direct extraction of hot carriers, or carrier multiplication.[35] For the hot carriers to be utilized efficiently, a slowed rate of carrier relaxation is desirable. Consequently, the majority of work in this area has focused on confined semiconductor quantum dots (QDs), where the quantization of states is predicted to impede carrier relaxation.[36] Both concepts were first demonstrated in small PbSe QDs,[37,38] and have recently been demonstrated as a proof-of-principle in LHP NC systems.[39–42] These studies have been accompanied by investigations into the relaxation dynamics of hot carriers. Although the reported lifetimes somewhat vary, the slowed cooling of hot carriers at high excitation conditions has been widely observed in LHP-based materials through transient absorption and photoluminescence (PL)

methods.[15,43–49] Early reports by Price et al.[43] and Yang et al.[44] connected this phenomenon to the "hot phonon bottleneck" mechanism that has been previously outlined for other traditional semiconductors.[50,51] Frost et al. explain this mechanism by considering the shared phonon subpopulation of optical phonons between spatially overlapping hot polaron states.[52] Following this work, we recently identified the cation as the key material parameter which controls this behavior in LHPs, as evidenced by our observation of more pronounced hot carrier density-dependent cooling in $CsPbBr_3$ with respect to the hybrid systems containing organic cations.[53] These findings are supported by other experimental and theoretical reports of cation-dependent carrier cooling in LHPs.[26,47,48,54]

Although there have been numerous studies on the dynamics of hot carriers in LHP-based materials, the explicit role of the cold carriers (band-edge states) on this process has been largely neglected. Advanced ultrafast two-dimensional electronic spectroscopy experiments have reported rapid carrier-carrier scattering and equilibration processes on sub-100 fs timescales after photoexcitation,[9,10] comparable to other semiconductors.[55] For high intensity photoexcitation, interactions between the cold and hot carriers are understood to occur in the process of Auger recombination, where the interband recombination of one (cold) electron-hole pair can re-excite an adjacent carrier.[56] These two scenarios present opposing effects of the cold carriers on the hot carrier dynamics in LHP materials, and serve to portray a complicated picture of energy redistribution following the generation of these states by the same excitation event. Similarly, the effects of electronic confinement and carrier trapping on carrier relaxation in LHPs are still under debate, not least because of the elaborate photophysics which occur in these materials and inhibit the contributions of specific effects toward carrier cooling from being studied in a controlled and isolated fashion.[26,57–59]

In this work, we evaluate the impact of the hot and cold carriers, as well as surface and confinement effects, on the hot carrier relaxation dynamics in LHP NC solids. For this we apply a three-pulse "pump-push-probe" (PPP) experiment, where the density of the hot and cold carrier subensembles are individually controlled. The results show that at low pump intensity (low cold carrier concentration), the hot carrier cooling dynamics exhibit a strong dependence on the number of optically re-excited carriers, which we ascribe to a phonon bottleneck mechanism in accordance with our previous findings.[53] Raising the pump intensity (cold carrier concentration) diminishes the dependence of the cooling dynamics on the number of hot states, pointing to a parallel relaxation process connected to the cold carriers. The identical density dependence of cooling rates for NCs with different ligands, and the similarity between the bulk and NC samples appear to preclude the effect of trap states and material interfaces, as well as weak electronic confinement on the hot carrier relaxation. These findings highlight the unique electronic properties of these materials systems and their tolerance towards defects with respect to conventional semiconductor materials.

Figure 1(a) shows the linear absorption and steady-state PL spectra for films of ~8 nm edge length $CsPbBr_3$ NCs following an established synthesis procedure incorporating the long chain zwitterion 3-N,N (dimethyloctadecylammonio)propansulfonate, referred to hereafter as "ZI", as the capping ligand.[60] The absorption onset and PL maxima of the NCs are both blueshifted with respect to bulk $CsPbBr_3$ (and indeed larger $CsPbBr_3$ NCs, as shown in Figure S1), which can be attributed to weak quantum confinement of the electronic states (for reference, the Bohr diameter of $CsPbBr_3$ is ~7 nm).[2] These dropcast NCs are moderately emissive (PL quantum yield ~60%) and monodisperse (PL linewidth ~26 nm), and share almost identical PL properties to the NCs suspended in solution (Figure S2). The size (average edge length ~8±2 nm)

and cuboid shape of these NCs was confirmed by transmission electron microscopy (TEM), shown in Figure 1(b).

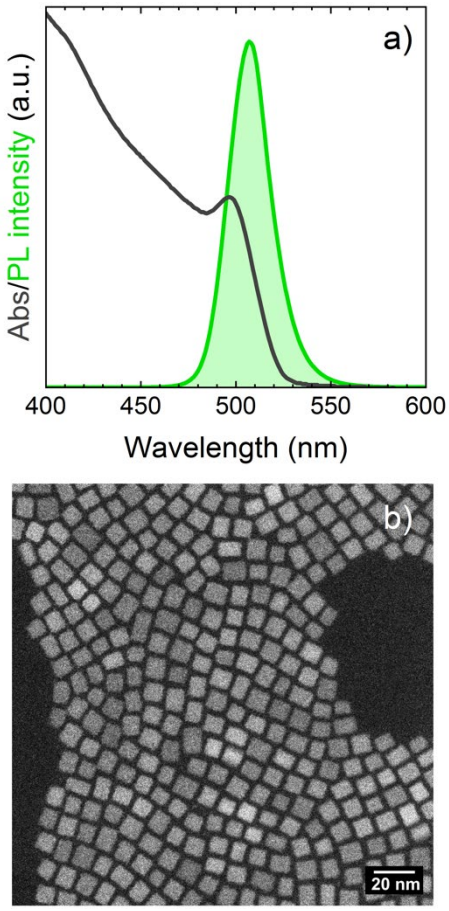


***Figure 1.*** *(a) Thin-film UV-Vis absorption and steady-state PL spectra of the dropcast ZI-capped $CsPbBr_3$ NCs. FWHM = 26 nm. The PL excitation was at 400 nm. (b) High-angle annular dark field scanning transmission electron micrograph (HAADF-STEM) of the ZI-capped $CsPbBr_3$ NCs with an average edge length of 8±2 nm collected at 77 K.*

In order to measure the carrier cooling in the samples, we employ a three-pulse differential transmission measurement, which we term "pump-push-probe" (PPP). Variants of this method have been used over the years to study a wide range of photophysical phenomena,

including photoionization dynamics in water,[61] charge delocalization in organic photovoltaic blends,[62] and indeed, carrier cooling in NCs.[63–65] The reader is directed to our recent work on bulk LHPs for the full details of the experiment used herein.[53] Briefly, a colinear visible (500 nm) "pump" and near-IR (2.1 μm) "probe" are focused onto the sample in order to generate carriers and subsequently monitor their photoinduced absorption.[66] After a 12 ps delay, the cold (band-edge) carriers are optically re-excited by an intense 2.1 μm "push" pulse, thereby bleaching the intraband absorption of the probe. The recovery of the pump-probe (PP) signal is interpreted as the cooling of the hot carriers, which we fit with a monoexponential function, with lifetime "$\tau_{cool}$". Figure 2(a) depicts the action of the pulses on the differential probe transmission through a thin film of the dropcast $CsPbBr_3$ NCs.

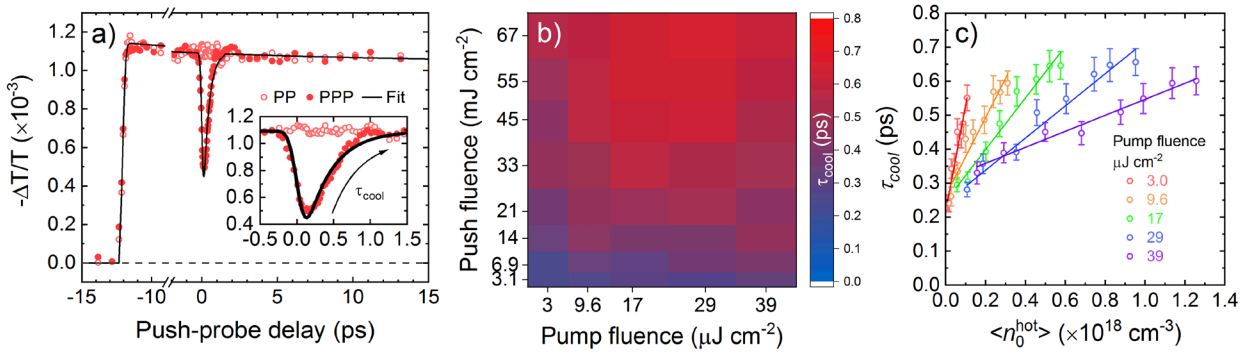


***Figure 2.*** *(a) Pump-probe (PP) and pump-push-probe (PPP) differential transmission transients for the dropcast 8 nm diameter ZI-capped $CsPbBr_3$ NCs. Pump: 500 nm, (3 μJ cm$^{-2}$); push: 2.1 μm (45 mJ cm$^{-2}$); probe: 2.1 μm. The inset depicts the extracted intraband cooling time, $\tau_{cool}$. The solid line is a Gaussian-convoluted monoexponential fit. (b) Pseudo-color map describing the dependence of $\tau_{cool}$ on the pump and push fluence. (c) $\tau_{cool}$ as a function of the average initial hot carrier density, $<n_0^{hot}>$, plotted for different pump fluences. The solid lines are linear fits as a guide to the eye.*

The pump fluence controls the initial number of cold carriers. In Figure 2(a), a low fluence was used (3 μJ $cm^{-2}$, corresponding to an average of ~0.1 excitons per NC, assuming a Poisson distribution). Since we are working with densely-packed films rather than colloidal solutions, we cannot rule out the interactions between carriers and phonons in adjacent NCs. Compared to other NC systems, carriers in films of surface passivated ~11 nm $CsPbBr_3$ NCs have been shown to exhibit a high mobility and diffusion length by optical pump-terahertz probe studies.[67] We therefore treat the system in the same way as a bulk material film composed of nanocrystalline domains, and quantify the number of excited states using a continuous distribution model. This gives an average initial cold carrier density, $\langle n_0^{cold} \rangle$, of $1.1 \times 10^{-17}$ $cm^{-3}$. As shown below, the accurate description of the material photophysics by this model corroborates the presence of interactions between excited states localized on different NCs. The many-body dynamics following higher fluence excitation can be seen in Figure S3.

The push fluence controls the number of hot carriers that are re-excited from the band-edge. Without state-resolved methods, we cannot unambiguously assign the push (and probe) transition to the valence or conduction band,[68,69] but we expect that the push interacts with electrons and holes in the same way due to their similar effective masses in LHP NCs.[2] As shown in Figure S4, the extent of bleaching scales linearly with the push fluence, which indicates that no more than one 2.1 μm photon is needed to excite a single cold carrier and bleach the probe transition.

Figure 2(b) presents the dependence of $\tau_{cool}$ on the pump and push intensities in a pseudo-color map. It is evident that there is a non-trivial connection between the dynamics of intraband relaxation and the relative number of cold and hot carriers. Figure 2(c) shows the dependence of $\tau_{cool}$ on both the pump fluence and the average initial density of hot carriers, $\langle n_0^{hot} \rangle$ (related to

the push fluence, see supporting notes for details). For all the data sets, regardless of the pump fluence (number of initial cold carriers), $\tau_{cool}$ is observed to increase with $<n_0^{hot}>$. Using the PPP technique, we previously attributed this underlying behavior to a hot phonon bottleneck mechanism; as the density of hot carriers increases, so does the competition for a finite number of phonon modes involved in cooling.[53] This phenomenon was also reported in other works employing more traditional PP methods.[15,43–49] To the best of our knowledge, no techniques to date have explicitly demonstrated the change in $\tau_{cool}$ upon the addition of cold carriers to the system. Figure 2(c) shows that as the pump intensity increases, the dependence of $\tau_{cool}$ on $<n_0^{hot}>$ is reduced, which can be observed as a flattening of the slope. This indicates the emergence of an additional mechanism, connected to the relative number of cold states, which accelerates the rate of carrier cooling in the NCs.

To explain the interplay between the phonon and cold-carrier mediated relaxation processes, we invoke the dual pathway model depicted in Figure 3. In order to reconcile the observation of weak confinement with the assumption of moderate electronic coupling, the electronic structure of the NCs is represented as a band composed of an inhomogenous density of states. Similar pictures have been used elsewhere for assembled QD solids.[70,71] Hot carriers in the LHP NCs can relax via two processes; (1) via scattering with longitudinal optical (LO) phonons, or; (2) via energy deposition into the cold carriers. While the detailed discussion of the model, approximations and the equations describing the spectroscopic data can be found elsewhere,[72] the equation describing the population of hot carriers as a function of time $n_H$(t) can be written in a concise and intuitive way:

$$\frac{\mathrm{d}n_H}{\mathrm{d}t} = -\alpha N_C n_H - \rho\gamma \exp(-\gamma N_H)\, n_H$$

Here $N_C$ represents the cold carrier density immediately before the arrival of push pulse, and $N_H$ represents the hot carrier density after the push pulse. $\alpha$, $\rho$ and $\gamma$ are constants reflecting carrier-carrier coupling, carrier-phonon coupling and the polaron volume, respectively. In the case where the carrier-carrier interactions (first term) are neglected and $\gamma N_H$ is small, the cooling time is given by:[72]

$$\tau \approx \frac{1}{\rho\gamma} + \frac{N_H}{\rho}$$

This rationalizes the underlying positive linear trend observed for all the data sets in Figure 2(c). This linear trend can also be explained phenomenologically, as $\tau_{cool}$ should be proportional to the overlapping volume of polarons associated with the hot carriers. As more hot polarons are added, their overlapping volume is expected to increase linearly (at least until overlaps of ≥3 polarons become dominant). When these hot polarons are generated in an environment containing many cold carriers, there is a greater probability for hot and cold carriers (polarons) to encounter one another. In this circumstance, cooling can occur via an Auger-type energy exchange, where the excess energy from an initial hot carrier is transferred to other cold carriers. This energy transfer mechanism should not be confused with a different Auger-type process that is known to occur in II-VI NCs such as CdSe QDs, where a dense manifold states close to the valence band maxima engenders an efficient transfer of excess electron energy into a hole.[73] The electronic properties of the LHP NCs are not conducive towards this relaxation pathway, since electrons and holes in these materials have small and almost equal effective masses.[2]

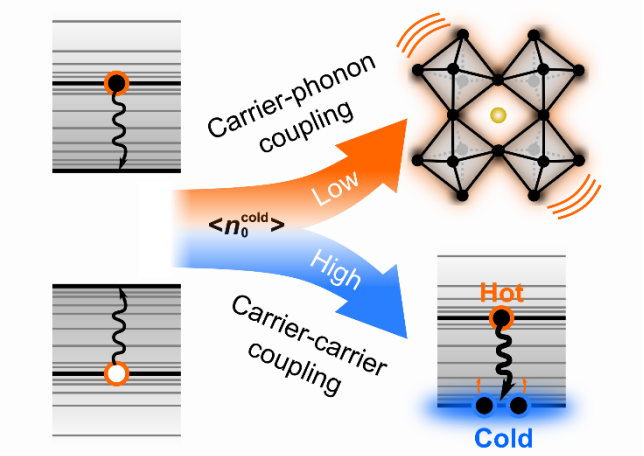


***Figure 3.*** *Schematic model to show the key cooling pathways available to the hot carriers in the LHP NCs. When the relative number of cold carriers is low, hot carriers cool via coupling to lattice vibrations. At higher cold carrier concentration, the exchange of energy between the hot and cold carrier ensembles via carrier-carrier coupling is dominant.*

So far, we have identified the overall role of carrier-phonon and carrier-carrier interactions on carrier cooling in the LHP NCs. However, in NCs, there are many material-specific relaxation channels which can compete with one another.[69] To check for other parameters that may be neglected by our proposed model, we studied carrier cooling in LHP NCs of different composition, size and surface treatment. To enhance the contrast between the studied systems, we performed the measurements at a low cold carrier density, where the effect of the carrier-phonon interaction is maximized. Figure 4(a) clearly demonstrates that, in comparison to $CsPbBr_3$ NCs, the dependence of $\tau_{cool}$ on the relative number of hot carriers is weaker in $FAPbBr_3$ NCs of a similar size (~10 nm, see Figure S1 for optical spectra and TEM images) and under similar pump conditions (~3 μJ $cm^{-2}$, see Figure S3 for fluence-dependent PP kinetics). The observation of faster overall cooling in the hybrid LHP system with respect to the all-inorganic $CsPbBr_3$ NCs is congruent with our recent findings,[53] as well as other experimental[26,47,48] and theoretical works.[54] We attribute the faster cooling behavior in the hybrid

LHP NCs to the higher density of phonon modes associated with the symmetry-breaking organic cation.[53]

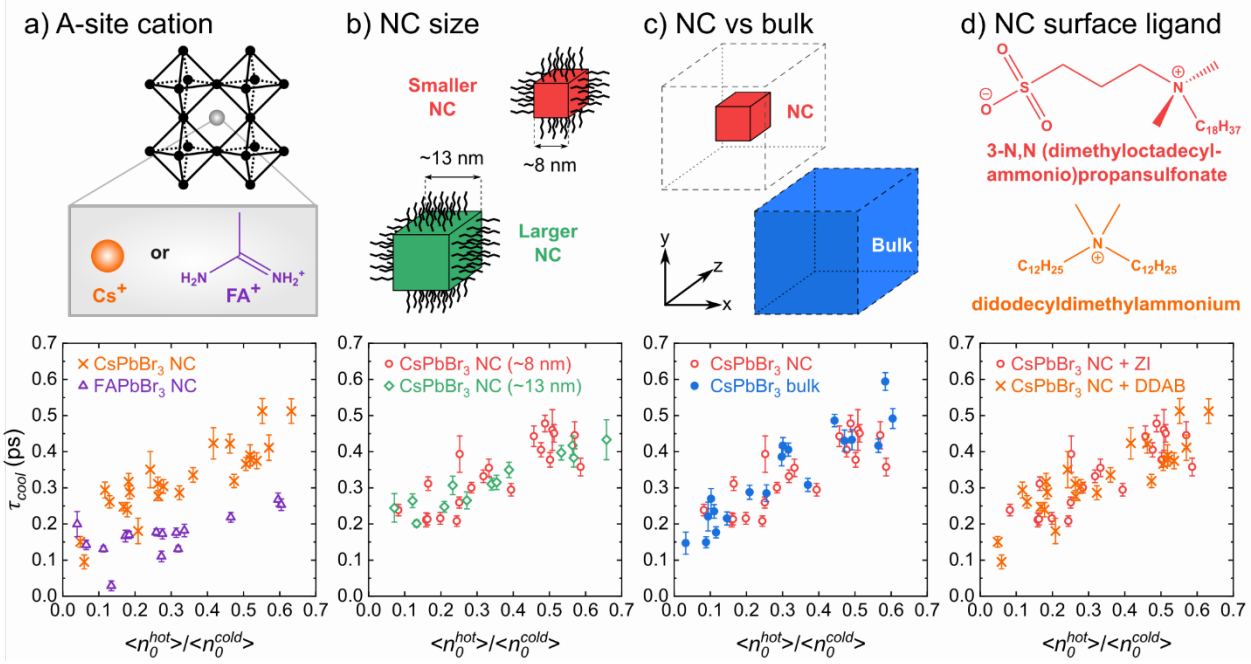


***Figure 4.*** *Dependence of carrier cooling lifetime on the density of hot carriers (just after the push), normalized by the density of cold carriers (just before the push), comparing (a) different cation composition for a given NC size (~10 nm) and surface ligand (DDAB), (b) different NC sizes (with the same ZI ligand), (c) bulk vs ~ 8 nm NC, and (d) NC capping ligands.*

Figure 4(b) does not show any obvious difference in the density-dependent cooling behavior for differently sized $CsPbBr_3$ NCs. Although the NCs studied herein are quite large, the optical characteristics of the smaller NCs are noticeably blue-shifted with respect to the larger NCs (Figure S1). While some studies in the literature have alluded to prolonged hot carrier lifetimes in smaller LHP NCs,[39] there is growing evidence to suggest that most weakly-confined LHP NCs exhibit only a very modest size dependence on carrier cooling.[47,74–76] As a side note, it is worth pointing out that the latter studies were performed in the solution phase, which indicates

that the rapid cooling we observe herein is not unique to solid films. With the exception of a few notable cases,[77] most studies on confined NCs show that the experimental rate of cooling is comparable to, or even faster, than the rate of cooling in the corresponding bulk material,[63,78,79] despite earlier predictions to the contrary.[36] Figure 4(c) shows identical cooling behavior for the $CsPbBr_3$ NC sample and a bulk $CsPbBr_3$ film, suggesting the absence of any noticeable confinement effects on carrier cooling in our samples. From this comparison, we can also conclude that any modification of the electron-hole interaction imposed by the NCs[80] does not significantly influence the cooling dynamics in the LHPs.

Changing the size of the NCs not only affects the confinement of the excited states, but also results in a different surface area-to-volume ratio. The fact that we observe similar cooling dynamics for NCs of different size indicates that surface states do not play a key role in the carrier relaxation. To verify this, we performed experiments on $CsPbBr_3$ NCs passivated with different ligands; ZI and didodecylammonium bromide (DDAB). Both ligands incorporate long hydrophobic chains, but are distinct in that the former can simultaneously coordinate to cationic and anionic sites on the LHP surface, which manifests itself as a higher PLQY of the films (see Figure S1) and reduced sintering of the NCs.[60,81] In spite of their different emission yields, Figure 4(d) shows that the overall cooling behavior in the ZI- and DDAB-capped $CsPbBr_3$ NCs is identical. This tentatively suggests that any defects which impinge upon the emission of the samples (particularly in the latter case) do not interfere with the intraband relaxation of the hot carriers. Furthermore, in comparing bulk and NC $CsPbBr_3$ in Figure 4(c), the additional interfaces (and any associated defects) imparted by the NCs do not seem to accelerate cooling.

We note that while some works have indicated the deleterious role of trap states and poor material quality on the dynamics of cooling in LHPs,[11,82,83] our method of intraband probing

ought to be sensitive to these effects. Using a similar experimental approach to our own, Guyot-Sionnest et al. demonstrated the direct effect of different surface treatments on the cooling dynamics in CdSe NCs.[63] The absence of defect-assisted carrier cooling herein is compatible with the results of other ultrafast experiments on LHP materials,[23,84–86] and is consistent with the widely-accepted consensus of defect tolerance for LHPs.[7,8] This may be attributed to the polaronic nature of charge carriers in these materials,[24–27,52,87] and could also be related to the low curvature and efficient packing of the cuboid LHP NCs which, in combination with the ligands, inhibits surface defect formation. On the subject of ligand effects, Guyot-Sionnest and coworkers have also proposed that direct energy transfer from the NC core to high-frequency ligand vibrations could play a role in intraband relaxation.[88] Clearly, we do not find evidence for this in comparing the DDAB and ZI-capped LHP NCs here (respective IR spectra can be found elsewhere[89,90]), and other works on carrier cooling in $CsPbBr_3$ NCs with more vibrationally distinct ligands have also ruled out this pathway.[75]

In conclusion, using a highly specialized "pump-push-probe" technique, we demonstrate the explicit effect of the hot and cold carriers on the carrier relaxation dynamics in lead-halide perovskite (LHP) nanocrystals (NCs). The hot and cold carrier subensembles affect the cooling dynamics in opposite ways. When the relative number of hot states is high, the time constant for cooling is observed to increase, which we interpret through a hot phonon bottleneck mechanism, where high energy carriers must compete for vibrational modes in order to cool. As the relative number of cold states increases, this density-dependent cooling behavior is observed to decrease. We rationalize this by invoking an additional pathway for cooling, where the excess energy of the hot carriers is preferentially deposited into the band-edge states as opposed to available phonon modes. We observe identical density-dependent cooling behavior when comparing NCs

of different sizes, and NCs with their bulk analogues. These factors portray the lack of electronic confinement effects on the carrier cooling dynamics, and moreover suggest that the additional material interfaces introduced in the nanocrystalline samples do not facilitate the relaxation of hot carriers. On a similar note, we also do not observe any appreciable difference in the cooling kinetics of LHP NCs with different capping ligands, further indicating that the surface of these materials is not essential for mediating hot carrier cooling. Our findings provide extensive insight into the interplay of carrier relaxation mechanisms in LHPs, which may be useful for the prospective development of high-performance technologies that utilize hot carriers. Furthermore, the findings emphasize the unique electronic and phononic properties of LHP NCs with respect to other semiconductor nanomaterials.

## ASSOCIATED CONTENT

### Supporting Information

The Supporting Information is available free of charge.

Experimental methods. Absorption and PL spectra for the NC films and solutions. Electron micrographs for all NC samples. Fluence-dependent pump-probe data for NC samples. Push fluence-dependent bleach kinetics.

## AUTHOR INFORMATION


### Corresponding Author

*Email: a.bakulin@imperial.ac.uk

### ORCID

Thomas R. Hopper: 0000-0001-5084-1914

Andrei Gorodetsky: 0000-0001-5440-2185

Franziska Krieg: 0000-0002-0370-1318

Maryna I. Bodnarchuk: 0000-0001-6597-3266

Marios Maimaris: 0000-0003-3474-9565

Thomas J. Macdonald: 0000-0002-7520-6893

Robert Lovrincic: 0000-0001-5429-5586

Maksym V. Kovalenko: 0000-0002-6396-8938

Artem A. Bakulin: 0000-0002-3998-2000

**Author Contributions**

T.R.H. and A.A.B. conceived the ultrafast experiments. T.R.H and A.G. built the ultrafast experimental setup. T.R.H., A.G., M.M. and M.C. performed the ultrafast spectroscopy measurements. T.R.H., A.G., A.J., M.M. and A.A.B. performed the analysis of the ultrafast spectroscopy data. F.K., M.I.B., X.H. synthesized and characterized the materials under the supervision of R.L. and M.B. T.R.H., M.C. and T.J.M. prepared the samples for spectroscopy measurements. The manuscript was written by T.R.H. through contributions of all authors. All authors have given approval to the final version of the manuscript.

**Notes**

The authors declare no competing financial interest.

ACKNOWLEDGMENTS

The authors thank Dr. Frank Krumeich for performing the HAADF-STEM measurements. M.V.K. acknowledges financial support from the Swiss Federal Commission for Technology and Innovation (CTI-No. 18614.1 PFNM-NM) and, in part, by the European Union through Horizon 2020 research and innovation programme (Grant Agreement No. 819740, project SCALE-HALO). A.A.B. is a Royal Society University Research Fellow. This project has also received funding from the European Research Council (ERC) under the European Union's Horizon 2020 research and innovation programme (Grant Agreement No. 639750).

REFERENCES

(1) Kovalenko, M. V.; Protesescu, L.; Bodnarchuk, M. I. Properties and Potential Optoelectronic Applications of Lead Halide Perovskite Nanocrystals. *Science* **2017**, *358* (6364), 745–750.

(2) Protesescu, L.; Yakunin, S.; Bodnarchuk, M. I.; Krieg, F.; Caputo, R.; Hendon, C. H.; Yang, R. X.; Walsh, A.; Kovalenko, M. V. Nanocrystals of Cesium Lead Halide Perovskites (CsPbX(3), X = Cl, Br, and I): Novel Optoelectronic Materials Showing Bright Emission with Wide Color Gamut. *Nano Lett.* **2015**, *15* (6), 3692–3696.

(3) Zhang, Y.; Liu, J.; Wang, Z.; Xue, Y.; Ou, Q.; Polavarapu, L.; Zheng, J.; Qi, X.; Bao, Q. Synthesis, Properties, and Optical Applications of Low-Dimensional Perovskites. *Chem. Commun.* **2016**, *52* (94), 13637–13655.

(4) Liu, F.; Zhang, Y.; Ding, C.; Kobayashi, S.; Izuishi, T.; Nakazawa, N.; Toyoda, T.; Ohta, T.; Hayase, S.; Minemoto, T.; et al. Highly Luminescent Phase-Stable CsPbI 3 Perovskite Quantum Dots Achieving Near 100% Absolute Photoluminescence Quantum Yield. *ACS Nano* **2017**, *11* (10), 10373–10383.

(5) Yakunin, S.; Protesescu, L.; Krieg, F.; Bodnarchuk, M. I.; Nedelcu, G.; Humer, M.; De Luca, G.; Fiebig, M.; Heiss, W.; Kovalenko, M. V. Low-Threshold Amplified Spontaneous Emission and Lasing from Colloidal Nanocrystals of Caesium Lead Halide Perovskites. *Nat. Commun.* **2015**, *6* (1), 8056.

(6) Park, Y.-S.; Guo, S.; Makarov, N. S.; Klimov, V. I. Room Temperature Single-Photon Emission from Individual Perovskite Quantum Dots. *ACS Nano* **2015**, *9* (10), 10386–10393.

(7) Huang, H.; Bodnarchuk, M. I.; Kershaw, S. V.; Kovalenko, M. V.; Rogach, A. L. Lead Halide Perovskite Nanocrystals in the Research Spotlight: Stability and Defect Tolerance. *ACS Energy Lett.* **2017**, *2* (9), 2071–2083.

(8) ten Brinck, S.; Zaccaria, F.; Infante, I. Defects in Lead Halide Perovskite Nanocrystals: Analogies and (Many) Differences with the Bulk. *ACS Energy Lett.* **2019**, acsenergylett.9b01945.

(9) Richter, J. M.; Branchi, F.; Valduga de Almeida Camargo, F.; Zhao, B.; Friend, R. H.; Cerullo, G.; Deschler, F. Ultrafast Carrier Thermalization in Lead Iodide Perovskite Probed with Two-Dimensional Electronic Spectroscopy. *Nat. Commun.* **2017**, *8* (1), 376.

(10) Ghosh, T.; Aharon, S.; Etgar, L.; Ruhman, S. Free Carrier Emergence and Onset of Electron–Phonon Coupling in Methylammonium Lead Halide Perovskite Films. *J. Am. Chem. Soc.* **2017**, *139* (50), 18262–18270.

(11) Kahmann, S.; Shao, S.; Loi, M. A. Cooling, Scattering, and Recombination—The Role of the Material Quality for the Physics of Tin Halide Perovskites. *Adv. Funct. Mater.* **2019**, *29* (35), 1902963.

(12) Saba, M.; Cadelano, M.; Marongiu, D.; Chen, F.; Sarritzu, V.; Sestu, N.; Figus, C.; Aresti, M.; Piras, R.; Geddo Lehmann, A.; et al. Correlated Electron–Hole Plasma in Organometal Perovskites. *Nat. Commun.* **2014**, *5* (1), 5049.

(13) Chen, X.; Lu, H.; Yang, Y.; Beard, M. C. Excitonic Effects in Methylammonium Lead Halide Perovskites. *J. Phys. Chem. Lett.* **2018**, *9* (10), 2595–2603.

(14) Eperon, G. E.; Jedlicka, E.; Ginger, D. S. Biexciton Auger Recombination Differs in Hybrid and Inorganic Halide Perovskite Quantum Dots. *J. Phys. Chem. Lett.* **2018**, *9* (1), 104–109.

(15) Mondal, A.; Aneesh, J.; Kumar Ravi, V.; Sharma, R.; Mir, W. J.; Beard, M. C.; Nag, A.; Adarsh, K. V. Ultrafast Exciton Many-Body Interactions and Hot-Phonon Bottleneck in Colloidal Cesium Lead Halide Perovskite Nanocrystals. *Phys. Rev. B* **2018**, *98* (11), 115418.

(16) Trinh, M. T.; Wu, X.; Niesner, D.; Zhu, X.-Y. Many-Body Interactions in Photo-Excited Lead Iodide Perovskite. *J. Mater. Chem. A* **2015**, *3* (17), 9285–9290.

(17) Juarez-Perez, E. J.; Sanchez, R. S.; Badia, L.; Garcia-Belmonte, G.; Kang, Y. S.; Mora-Sero, I.; Bisquert, J. Photoinduced Giant Dielectric Constant in Lead Halide Perovskite Solar Cells. *J. Phys. Chem. Lett.* **2014**, *5* (13), 2390–2394.

(18) Even, J.; Pedesseau, L.; Katan, C. Analysis of Multivalley and Multibandgap Absorption and Enhancement of Free Carriers Related to Exciton Screening in Hybrid Perovskites. *J. Phys. Chem. C* **2014**, *118* (22), 11566–11572.

(19) Anusca, I.; Balčiūnas, S.; Gemeiner, P.; Svirskas, Š.; Sanlialp, M.; Lackner, G.;

Fettkenhauer, C.; Belovickis, J.; Samulionis, V.; Ivanov, M.; et al. Dielectric Response: Answer to Many Questions in the Methylammonium Lead Halide Solar Cell Absorbers. *Adv. Energy Mater.* **2017**, *7* (19), 1700600.

(20) Wright, A. D.; Verdi, C.; Milot, R. L.; Eperon, G. E.; Pérez-Osorio, M. A.; Snaith, H. J.; Giustino, F.; Johnston, M. B.; Herz, L. M. Electron-Phonon Coupling in Hybrid Lead Halide Perovskites. *Nat. Commun.* **2016**, *7* (May).

(21) Iaru, C. M.; Geuchies, J. J.; Koenraad, P. M.; Vanmaekelbergh, D.; Silov, A. Y. Strong Carrier–Phonon Coupling in Lead Halide Perovskite Nanocrystals. *ACS Nano* **2017**, *11* (11), 11024–11030.

(22) Herz, L. M. How Lattice Dynamics Moderate the Electronic Properties of Metal-Halide Perovskites. *J. Phys. Chem. Lett.* **2018**, *9* (23), 6853–6863.

(23) Guzelturk, B.; Belisle, R. A.; Smith, M. D.; Bruening, K.; Prasanna, R.; Yuan, Y.; Gopalan, V.; Tassone, C. J.; Karunadasa, H. I.; McGehee, M. D.; et al. Terahertz Emission from Hybrid Perovskites Driven by Ultrafast Charge Separation and Strong Electron-Phonon Coupling. *Adv. Mater.* **2018**, *30* (11), 1704737.

(24) Zhu, H.; Miyata, K.; Fu, Y.; Wang, J.; Joshi, P. P.; Niesner, D.; Williams, K. W.; Jin, S.; Zhu, X.-Y. Y. Screening in Crystalline Liquids Protects Energetic Carriers in Hybrid Perovskites. *Science* **2016**, *353* (6306), 1409–1413.

(25) Evans, T. J. S.; Miyata, K.; Joshi, P. P.; Maehrlein, S.; Liu, F.; Zhu, X.-Y. Y. Competition Between Hot-Electron Cooling and Large Polaron Screening in CsPbBr 3 Perovskite Single Crystals. *J. Phys. Chem. C* **2018**, *122* (25), 13724–13730.

(26) Bretschneider, S. A.; Ivanov, I.; Wang, H. I.; Miyata, K.; Zhu, X.; Bonn, M. Quantifying Polaron Formation and Charge Carrier Cooling in Lead-Iodide Perovskites. *Adv. Mater.* **2018**, *0* (0), 1707312.

(27) Cinquanta, E.; Meggiolaro, D.; Motti, S. G.; Gandini, M.; Alcocer, M. J. P.; Akkerman, Q. A.; Vozzi, C.; Manna, L.; De Angelis, F.; Petrozza, A.; et al. Ultrafast THz Probe of Photoinduced Polarons in Lead-Halide Perovskites. *Phys. Rev. Lett.* **2019**, *122* (16), 166601.

(28) Stoumpos, C. C.; Malliakas, C. D.; Kanatzidis, M. G. Semiconducting Tin and Lead Iodide Perovskites with Organic Cations: Phase Transitions, High Mobilities, and Near-Infrared Photoluminescent Properties. *Inorg. Chem.* **2013**, *52* (15), 9019–9038.

(29) Quarti, C.; Mosconi, E.; Ball, J. M.; D'Innocenzo, V.; Tao, C.; Pathak, S.; Snaith, H. J.; Petrozza, A.; De Angelis, F. Structural and Optical Properties of Methylammonium Lead Iodide across the Tetragonal to Cubic Phase Transition: Implications for Perovskite Solar Cells. *Energy Environ. Sci.* **2016**, *9* (1), 155–163.

(30) Whalley, L. D.; Skelton, J. M.; Frost, J. M.; Walsh, A. Phonon Anharmonicity, Lifetimes, and Thermal Transport in CH3NH3PbI3 from Many-Body Perturbation Theory. *Phys. Rev. B* **2016**, *94* (22), 220301.

(31) Sendner, M.; Nayak, P. K.; Egger, D. A.; Beck, S.; Muller, C.; Epding, B.; Kowalsky, W.; Kronik, L.; Snaith, H. J.; Pucci, A.; et al. Optical Phonons in Methylammonium Lead Halide Perovskites and Implications for Charge Transport. *Mater. Horizons* **2016**, *3* (6), 613–620.

(32) Munson, K. T.; Swartzfager, J. R.; Asbury, J. B. Lattice Anharmonicity: A Double-Edged

Sword for 3D Perovskite-Based Optoelectronics. *ACS Energy Lett.* **2019**, 1888–1897.

(33) Kahmann, S.; Loi, M. A. Hot Carrier Solar Cells and the Potential of Perovskites for Breaking the Shockley–Queisser Limit. *J. Mater. Chem. C* **2019**.

(34) Shockley, W.; Queisser, H. J. Detailed Balance Limit of Efficiency of P-n Junction Solar Cells. *J. Appl. Phys.* **1961**, *32* (3), 510–519.

(35) Nelson, C. A.; Monahan, N. R.; Zhu, X.-Y. Exceeding the Shockley–Queisser Limit in Solar Energy Conversion. *Energy Environ. Sci.* **2013**, *6* (12), 3508.

(36) Bockelmann, U.; Bastard, G. Phonon Scattering and Energy Relaxation in Two-, One-, and Zero-Dimensional Electron Gases. *Phys. Rev. B* **1990**, *42* (14), 8947–8951.

(37) Tisdale, W. A.; Williams, K. J.; Timp, B. A.; Norris, D. J.; Aydil, E. S.; Zhu, X.-Y. Hot-Electron Transfer from Semiconductor Nanocrystals. *Science* **2010**, *328* (5985), 1543–1547.

(38) Schaller, R. D.; Klimov, V. I. High Efficiency Carrier Multiplication in PbSe Nanocrystals: Implications for Solar Energy Conversion. *Phys. Rev. Lett.* **2004**, *92* (18), 186601.

(39) Li, M.; Bhaumik, S.; Goh, T. W.; Kumar, M. S.; Yantara, N.; Grätzel, M.; Mhaisalkar, S.; Mathews, N.; Sum, T. C. Slow Cooling and Highly Efficient Extraction of Hot Carriers in Colloidal Perovskite Nanocrystals. *Nat. Commun.* **2017**, *8* (May), 14350.

(40) de Weerd, C.; Gomez, L.; Capretti, A.; Lebrun, D. M.; Matsubara, E.; Lin, J.; Ashida, M.; Spoor, F. C. M.; Siebbeles, L. D. A.; Houtepen, A. J.; et al. Efficient Carrier Multiplication in CsPbI3 Perovskite Nanocrystals. *Nat. Commun.* **2018**, *9* (1), 1–3.

(41) Manzi, A.; Tong, Y.; Feucht, J.; Yao, E.-P.; Polavarapu, L.; Urban, A. S.; Feldmann, J. Resonantly Enhanced Multiple Exciton Generation through Below-Band-Gap Multi-Photon Absorption in Perovskite Nanocrystals. *Nat. Commun.* **2018**, *9* (1), 1518.

(42) Li, M.; Begum, R.; Fu, J.; Xu, Q.; Koh, T. M.; Veldhuis, S. A.; Grätzel, M.; Mathews, N.; Mhaisalkar, S.; Sum, T. C. Low Threshold and Efficient Multiple Exciton Generation in Halide Perovskite Nanocrystals. *Nat. Commun.* **2018**, *9* (1), 4197.

(43) Price, M. B.; Butkus, J.; Jellicoe, T. C.; Sadhanala, A.; Briane, A.; Halpert, J. E.; Broch, K.; Hodgkiss, J. M.; Friend, R. H.; Deschler, F. Hot-Carrier Cooling and Photoinduced Refractive Index Changes in Organic–Inorganic Lead Halide Perovskites. *Nat. Commun.* **2015**, *6* (1), 8420.

(44) Yang, Y.; Ostrowski, D. P.; France, R. M.; Zhu, K.; van de Lagemaat, J.; Luther, J. M.; Beard, M. C. Observation of a Hot-Phonon Bottleneck in Lead-Iodide Perovskites. *Nat. Photonics* **2016**, *10* (1), 53–59.

(45) Piatkowski, P.; Cohen, B.; Kazim, S.; Ahmad, S.; Douhal, A. How Photon Pump Fluence Changes the Charge Carrier Relaxation Mechanism in an Organic–Inorganic Hybrid Lead Triiodide Perovskite. *Phys. Chem. Chem. Phys.* **2016**, *18* (39), 27090–27101.

(46) Yang, J.; Wen, X.; Xia, H.; Sheng, R.; Ma, Q.; Kim, J.; Tapping, P.; Harada, T.; Kee, T. W.; Huang, F.; et al. Acoustic-Optical Phonon up-Conversion and Hot-Phonon Bottleneck in Lead-Halide Perovskites. *Nat. Commun.* **2017**, *8*, 14120.

(47) Diroll, B. T.; Schaller, R. D. Intraband Cooling in All-Inorganic and Hybrid Organic–Inorganic Perovskite Nanocrystals. *Adv. Funct. Mater.* **2019**, *1901725*, 1901725.

(48) Chen, J.; Messing, M. E.; Zheng, K.; Pullerits, T. Cation Dependent Hot Carrier Cooling in Halide Perovskite Nanocrystals. *J. Am. Chem. Soc.* **2019**, jacs.8b11867.

(49) Papagiorgis, P.; Protesescu, L.; Kovalenko, M. V.; Othonos, A.; Itskos, G. Long-Lived Hot Carriers in Formamidinium Lead Iodide Nanocrystals. *J. Phys. Chem. C* **2017**, *121* (22), 12434–12440.

(50) Shah, J.; Leite, R. C. C. Radiative Recombination from Photoexcited Hot Carriers in GaAs. *Phys. Rev. Lett.* **1969**, *22* (24), 1304–1307.

(51) Shah, J. Hot Electrons and Phonons under High Intensity Photoexcitation of Semiconductors. *Solid. State. Electron.* **1978**, *21* (1), 43–50.

(52) Frost, J. M.; Whalley, L. D.; Walsh, A. Slow Cooling of Hot Polarons in Halide Perovskite Solar Cells. *ACS Energy Lett.* **2017**, *2* (12), 2647–2652.

(53) Hopper, T. R.; Gorodetsky, A.; Frost, J. M.; Müller, C.; Lovrincic, R.; Bakulin, A. A. Ultrafast Intraband Spectroscopy of Hot-Carrier Cooling in Lead-Halide Perovskites. *ACS Energy Lett.* **2018**, *3* (9), 2199–2205.

(54) Madjet, M. E.; Berdiyorov, G. R.; El-Mellouhi, F.; Alharbi, F. H.; Akimov, A. V; Kais, S. Cation Effect on Hot Carrier Cooling in Halide Perovskite Materials. *J. Phys. Chem. Lett.* **2017**, *8* (18), 4439–4445.

(55) Lyon, S. A. Spectroscopy of Hot Carriers in Semiconductors. *J. Lumin.* **1986**, *35* (3), 121–154.

(56) Herz, L. M. Charge-Carrier Dynamics in Organic-Inorganic Metal Halide Perovskites.

*Annu. Rev. Phys. Chem.* **2016**, *67* (1), 65–89.

(57) Manser, J. S.; Kamat, P. V. Band Filling with Free Charge Carriers in Organometal Halide Perovskites. *Nat. Photonics* **2014**, *8* (9), 737–743.

(58) Wang, L.; Brawand, N. P.; Vörös, M.; Dahlberg, P. D.; Otto, J. P.; Williams, N. E.; Tiede, D. M.; Galli, G.; Engel, G. S. Excitations Partition into Two Distinct Populations in Bulk Perovskites. *Adv. Opt. Mater.* **2018**, *6* (5), 1700975.

(59) Wei, K.; Zheng, X.; Cheng, X.; Shen, C.; Jiang, T. Observation of Ultrafast Exciton-Exciton Annihilation in CsPbBr 3 Quantum Dots. *Adv. Opt. Mater.* **2016**, *4* (12), 1993–1997.

(60) Krieg, F.; Ochsenbein, S. T.; Yakunin, S.; ten Brinck, S.; Aellen, P.; Süess, A.; Clerc, B.; Guggisberg, D.; Nazarenko, O.; Shynkarenko, Y.; et al. Colloidal CsPbX 3 (X = Cl, Br, I) Nanocrystals 2.0: Zwitterionic Capping Ligands for Improved Durability and Stability. *ACS Energy Lett.* **2018**, *3* (3), 641–646.

(61) Son, D. H.; Kambhampati, P.; Kee, T. W.; Barbara, P. F. Delocalizing Electrons in Water with Light. *J. Phys. Chem. A* **2001**, *105* (36), 8269–8272.

(62) Bakulin, A. A.; Rao, A.; Pavelyev, V. G.; Van Loosdrecht, P. H. M.; Pshenichnikov, M. S.; Niedzialek, D.; Cornil, J.; Beljonne, D.; Friend, R. H. The Role of Driving Energy and Delocalized States for Charge Separation in Organic Semiconductors. *Science* **2012**, *335* (6074), 1340–1344.

(63) Guyot-Sionnest, P.; Shim, M.; Matranga, C.; Hines, M. Intraband Relaxation in CdSe Quantum Dots. *Phys. Rev. B* **1999**, *60* (4), R2181–R2184.

(64) Rabouw, F. T.; Vaxenburg, R.; Bakulin, A. A.; van Dijk-Moes, R. J. A.; Bakker, H. J.; Rodina, A.; Lifshitz, E.; L. Efros, A.; Koenderink, A. F.; Vanmaekelbergh, D. Dynamics of Intraband and Interband Auger Processes in Colloidal Core–Shell Quantum Dots. *ACS Nano* **2015**, *9* (10), 10366–10376.

(65) Gdor, I.; Shapiro, A.; Yang, C.; Yanover, D.; Lifshitz, E.; Ruhman, S. Three-Pulse Femtosecond Spectroscopy of PbSe Nanocrystals: 1S Bleach Nonlinearity and Sub-Band-Edge Excited-State Absorption Assignment. *ACS Nano* **2015**, *9* (2), 2138–2147.

(66) Munson, K. T.; Grieco, C.; Kennehan, E. R.; Stewart, R. J.; Asbury, J. B. Time-Resolved Infrared Spectroscopy Directly Probes Free and Trapped Carriers in Organo-Halide Perovskites. *ACS Energy Lett.* **2017**, *2* (3), 651–658.

(67) Yettapu, G. R.; Talukdar, D.; Sarkar, S.; Swarnkar, A.; Nag, A.; Ghosh, P.; Mandal, P. Terahertz Conductivity within Colloidal CsPbBr 3 Perovskite Nanocrystals: Remarkably High Carrier Mobilities and Large Diffusion Lengths. *Nano Lett.* **2016**, *16* (8), 4838–4848.

(68) Kambhampati, P. Unraveling the Structure and Dynamics of Excitons in Semiconductor Quantum Dots. *Acc. Chem. Res.* **2011**, *44* (1), 1–13.

(69) Kambhampati, P. Hot Exciton Relaxation Dynamics in Semiconductor Quantum Dots: Radiationless Transitions on the Nanoscale. *J. Phys. Chem. C* **2011**, *115* (45), 22089–22109.

(70) Nozik, A. J. Spectroscopy and Hot Electron Relaxation Dynamics in Semiconductor Quantum Wells and Quantum Dots. *Annu. Rev. Phys. Chem.* **2001**, *52* (1), 193–231.

(71) Gao, Y.; Talgorn, E.; Aerts, M.; Trinh, M. T.; Schins, J. M.; Houtepen, A. J.; Siebbeles, L.

D. A. Enhanced Hot-Carrier Cooling and Ultrafast Spectral Diffusion in Strongly Coupled PbSe Quantum-Dot Solids. *Nano Lett.* **2011**, *11* (12), 5471–5476.

(72) Hopper, T. R.; Jeong, A.; Gorodetsky, A.; Krieg, F.; Bodnarchuk, M. I.; Huang, X.; Lovrincic, R.; Kovalenko, M. V.; Bakulin, A. A. Kinetic modelling of carrier cooling in lead halide perovskite materials http://arxiv.org/abs/1912.05354 (accessed Feb 25, 2020).

(73) Efros, A. L.; Kharchenko, V. A.; Rosen, M. Breaking the Phonon Bottleneck in Nanometer Quantum Dots: Role of Auger-like Processes. *Solid State Commun.* **1995**, *93* (4), 281–284.

(74) Butkus, J.; Vashishtha, P.; Chen, K.; Gallaher, J. K.; Prasad, S. K. K.; Metin, D. Z.; Laufersky, G.; Gaston, N.; Halpert, J. E.; Hodgkiss, J. M. The Evolution of Quantum Confinement in CsPbBr 3 Perovskite Nanocrystals. *Chem. Mater.* **2017**, *29* (8), 3644–3652.

(75) Li, Y.; Lai, R.; Luo, X.; Liu, X.; Ding, T.; Lu, X.; Wu, K. On the Absence of a Phonon Bottleneck in Strongly Confined CsPbBr 3 Perovskite Nanocrystals. *Chem. Sci.* **2019**, *10* (23), 5983–5989.

(76) Boehme, S. C.; ten Brinck, S.; Maes, J.; Yazdani, N.; Zapata, F.; Chen, K.; Wood, V.; Hodgkiss, J. M.; Hens, Z.; Geiregat, P.; et al. Phonon-Mediated and Weakly Size-Dependent Electron and Hole Cooling in CsPbBr 3 Nanocrystals Revealed by Atomistic Simulations and Ultrafast Spectroscopy. *Nano Lett.* **2020**, acs.nanolett.9b05051.

(77) Pandey, A.; Guyot-Sionnest, P. Slow Electron Cooling in Colloidal Quantum Dots. *Science* **2008**, *322* (5903), 929–932.

(78) Cooney, R. R.; Sewall, S. L.; Anderson, K. E. H.; Dias, E. A.; Kambhampati, P. Breaking

the Phonon Bottleneck for Holes in Semiconductor Quantum Dots. *Phys. Rev. Lett.* **2007**, *98* (17), 177403.

(79) Schaller, R. D.; Pietryga, J. M.; Goupalov, S. V.; Petruska, M. A.; Ivanov, S. A.; Klimov, V. I. Breaking the Phonon Bottleneck in Semiconductor Nanocrystals via Multiphonon Emission Induced by Intrinsic Nonadiabatic Interactions. *Phys. Rev. Lett.* **2005**, *95* (19), 196401.

(80) Castañeda, J. A.; Nagamine, G.; Yassitepe, E.; Bonato, L. G.; Voznyy, O.; Hoogland, S.; Nogueira, A. F.; Sargent, E. H.; Cruz, C. H. B.; Padilha, L. A. Efficient Biexciton Interaction in Perovskite Quantum Dots Under Weak and Strong Confinement. *ACS Nano* **2016**, *10* (9), 8603–8609.

(81) Bodnarchuk, M. I.; Boehme, S. C.; ten Brinck, S.; Bernasconi, C.; Shynkarenko, Y.; Krieg, F.; Widmer, R.; Aeschlimann, B.; Günther, D.; Kovalenko, M. V.; et al. Rationalizing and Controlling the Surface Structure and Electronic Passivation of Cesium Lead Halide Nanocrystals. *ACS Energy Lett.* **2019**, *4* (1), 63–74.

(82) Jiang, X.; Hoffman, J. M.; Stoumpos, C. C.; Kanatzidis, M. G.; Harel, E. Transient Sub-Bandgap States at Grain Boundaries of CH3NH3PbI3 Perovskite Act as Fast Temperature Relaxation Centers. *ACS Energy Lett.* **2019**, acsenergylett.9b00885.

(83) Zheng, K.; Žídek, K.; Abdellah, M.; Chen, J.; Chábera, P.; Zhang, W.; Al-Marri, M. J.; Pullerits, T. High Excitation Intensity Opens a New Trapping Channel in Organic–Inorganic Hybrid Perovskite Nanoparticles. *ACS Energy Lett.* **2016**, *1* (6), 1154–1161.

(84) Bretschneider, S. A.; Laquai, F.; Bonn, M. Trap-Free Hot Carrier Relaxation in Lead–

Halide Perovskite Films. *J. Phys. Chem. C* **2017**, *121* (21), 11201–11206.

(85) Ghosh, T.; Aharon, S.; Shpatz, A.; Etgar, L.; Ruhman, S. Reflectivity Effects on Pump–Probe Spectra of Lead Halide Perovskites: Comparing Thin Films versus Nanocrystals. *ACS Nano* **2018**, *12* (6), 5719–5725.

(86) Geiregat, P.; Maes, J.; Chen, K.; Drijvers, E.; De Roo, J.; Hodgkiss, J. M.; Hens, Z. Using Bulk-like Nanocrystals to Probe Intrinsic Optical Gain Characteristics of Inorganic Lead Halide Perovskites. *ACS Nano* **2018**, *12*, 10178–10188.

(87) Zhu, X.-Y.; Podzorov, V. Charge Carriers in Hybrid Organic–Inorganic Lead Halide Perovskites Might Be Protected as Large Polarons. *J. Phys. Chem. Lett.* **2015**, *6* (23), 4758–4761.

(88) Guyot-Sionnest, P.; Wehrenberg, B.; Yu, D. Intraband Relaxation in CdSe Nanocrystals and the Strong Influence of the Surface Ligands. *J. Chem. Phys.* **2005**, *123* (7), 074709.

(89) Sigma Aldrich, FT-IR spectrum of didecyldimethylammonium bromide https://www.sigmaaldrich.com/spectra/rair/RAIR007657.PDF (accessed Dec 9, 2019).

(90) Sigma Aldrich, FT-IR spectrum of 3-(N,N-Dimethyloctadecylammonio)propanesulfonate https://www.sigmaaldrich.com/spectra/rair/RAIR009927.PDF (accessed Dec 9, 2019).